CERN-TH.5571/89
DAMTP 89/28

A QCD-inspired model for exclusive vector meson production in deep inelastic scattering

J.R. Cudell
CERN, TH Division
CH 1211 Genève 23 Switzerland

ABSTRACT

Most of the features of the exclusive $\gamma^* p \to \rho^0 p$ signal can be reproduced by a simple model which extends perturbative QCD to small momentum transfers in a natural way while linking pomeron behaviour with the gluon condensate. The data, however, seem to exhibit features characteristic of inelastic distributions, even after subtraction of a possible inelastic background.

CERN-TH.5571
DAMTP 89/28
October 1989

Introduction

Many processes are well described by perturbative QCD, but once momentum transfers become small, the perturbative expansion breaks down. This happens not so much because of the size of the strong coupling constant, but rather because of the presence of soft divergences. However, although they cannot be justified theoretically, the perturbative QCD differential distributions still seem to describe the data up to "a factor", which often depends on an infrared cutoff. This suggests that it must be possible to extend perturbative QCD to the infrared region. This paper examines in detail the consequences of a model previously proposed[1], which regulates the infrared divergences in a process-independent way while staying as close as possible to perturbative QCD. Vector meson production is in fact a very good framework for testing such ideas, as the inclusive data seem to be well described[2] by a perturbative QCD calculation. We shall thus concentrate on the ideas proposed by Donnachie and Landshoff to explain the EMC ρ^0 exclusive data. Their first model[3], based on the analogy pomeron-photon was rather successful. Since then, Landshoff and Nachtmann[1] have succeeded, at $t = 0$, to describe the pomeron in terms of a modified tree-level two-gluon exchange, thus providing a connection with QCD. Landshoff and Donnachie have shown[4] that the pomeron trajectory could be obtained at non zero t, using the same tree-level gluon exchange. Ross has recently calculated[5] part of the higher-order corrections and confirmed that this model can indeed lead to a pomeron behaviour at non zero t, when resummed to higher orders, whereas perturbative QCD seems to fail in that respect. The original idea has since been modified to mimic colour while preserving the other results[6].

This paper carefully spells out the uncertainties attached to this model, presents its consequences in the context of ρ^0 exclusive production, where the background is carefully evaluated, and explains where the calculation breaks down, and why. The first section will briefly describe the framework used in the following, and the connection between the gluon propagator at small momentum transfer and the pomeron. More extensive descriptions have been published elsewhere[1,3,4,6]. These ideas are then applied to exclusive vector meson production, and the connection between the resulting picture and perturbative QCD is explained. A comparison with the Q^2 distribution of the exclusive signal suggests that the quark propagator does not need to be modified until one reaches very small momentum transfers, of the order of 500 MeV. The second section describes the procedure followed to mimic the experimental extraction of the photon cross-section. Special attention will be paid

to the possible inelastic background and to the uncertainties attached to its evaluation. The third section presents the results of a comparison of our results with the EMC data[7]. Reasonable agreement is reached. Two pieces of data still disagree with the model, namely the t slopes of the signal and the distributions violating helicity conservation. It is possible to ascribe the latter problem to uncertainties in the experimental analysis. On the other hand, the t slopes are shown to be characteristic of a wide class of inclusive distributions, but seem to be incompatible with an exclusive signal.

1. Non perturbative model

The basic idea is that the infrared singularities present in perturbative QCD can be regulated in a process independent way. They arise from the singularity of the gluon propagator $D(l^2)$ at $l^2 = 0$, and thus this quantity has to be modified when $|l^2|$ becomes small. How to do this can be guessed at by considering first the total cross section: high energy behaviour should be obtained from the exchange of two gluons with a modified propagator. That is to say that such an exchange must produce hadronic amplitudes that behave like s^1 at high centre of mass energy $\sqrt{s}$, and must be such that the total cross section for the interaction of hadrons A and B will be proportional to the product of the number of quarks n_A and n_B present in each hadron. This leads to two requirements[1]: i) the gluon propagator should be finite at $l^2=0$, and this introduces a correlation length a, which should be small compared to a typical hadronic radius R, and ii) the magnitude of the two gluon exchange should reproduce the magnitude of the total cross section. This can be translated into:

$$2\pi \int_{-\infty}^{0} dl^2 \alpha_\pi^2 D^2(l^2) = \frac{9}{2}\beta_0^2 \qquad (1)$$

with α_π the coupling constant in the non perturbative regime, and $\beta_0^2 = 3.93\ \mathrm{GeV}^{-2}$.

One can then use gluon condensate estimates to further constrain the answer, thus linking the model with non perturbative QCD. This leads to a second moment of the gluon propagator:

$$\int_{-\infty}^{0} dl^2\, l^4 \alpha_\pi D(l^2) = \frac{2\pi}{3} M_c^4 \qquad (2)$$

with $M_c^4 = \langle 0 | 4\pi\, \alpha_\pi G^{\mu\nu}(0)\, G_{\mu\nu}(0) | 0 \rangle \approx (1\ \mathrm{GeV}^4)$. One unfortunately has to neglect non abelian terms to derive this expression, so that this second moment is not absolutely reliable. We shall consider the uncertainties attached to its modification in the following.

The simplest choice that satisfies both these requirements is:

$$\text{for } k^2 \le 0 : \alpha_\pi D(l^2) = \frac{3\beta_0}{\sqrt{2\pi}\,\mu_0} \exp\left(\frac{l^2}{\mu_0^2}\right) \qquad (3)$$

with μ_0=1.1 GeV. α_n is the strength of the non perturbative coupling, which is assumed independent of l^2. As we shall explain below, the exact form of the propagator is not of extreme importance for this calculation (although it matters when higher orders are included).

Equation (3) describes the gluon propagator at small l^2. For large momentum transfers, the usual $1/l^2$ has to be kept as its consequences are experimentally verified. The propagator must then turn smoothly from one functional form to the other. The perturbative and the non perturbative propagators cross at a point $l^2=Q_0^2$. We shall assume that below Q_0^2 the propagator is described by (3), whereas above Q_0^2 the usual $1/l^2$ holds. We shall also assume that the coupling constant gets frozen at that scale, so that $\alpha_n=\alpha_S(Q_0^2)$. This prescription is of course only a best guess. Figure 1 shows the values of Q_0^2 and of α_n that result from it, as functions of μ_0 and of Λ_{QCD}. One sees that α_n≈0.2 to 0.5, which are values compatible with those needed to get a sensible answer for the gluon structure function at small x[6]. Finally, it has been shown[6] that when a modified gluon couples to a far off-shell quark of off-shellness κ^2, the coupling is $\alpha_S(\kappa^2)$.

After this brief summary, we can now turn explicitly to the process $\gamma p \rightarrow \rho^0 p$. We want to stress here that the model that we used has been derived independently of this process, and that this study provides a real test for it.

We use in the following standard notation for deep-inelastic scattering: q, V, P and P' are the 4-momenta respectively of the photon, the vector meson, the incoming proton and the scattered hadrons (proton in the exclusive case). As usual $\nu=p\cdot q/m$, $Q^2=-q^2$, $t=(P-P')^2$, $z=P\cdot V/P\cdot q$, $w^2=(P+q)^2$, m_p is the proton mass, m_V is the vector meson mass and V_T is the transverse momentum of the vector meson with respect to the q axis.

The inclusive distributions are well described by a perturbative QCD calculation when V_T is large (≥ 0.6 GeV) and z small (≤0.95) [2]. The basic assumption of the model is that at high Q^2, vector meson production is a short-range process, and that the vector meson is adequately described by a non-relativistic wave function, i.e. that it interacts via its two constituent quarks, and that these carry half of its 4-momentum each. This should be valid as long as Q^2 is large enough for the probe to be much smaller than the meson size. The vertex $q\bar{q} \rightarrow \rho^0$ can be normalized via the process $\rho^0 \rightarrow e^+e^-$, and the vertex function becomes:

$$U(V) = \Phi(\gamma . V + m_V)$$
$$\text{with } \Phi = \sqrt{\frac{f_V m_V}{24}} \qquad (4)$$

f_V is measured experimentally to be (30 ± 4) MeV for ρ^0 [8].

At moderate V_T and for large z, the perturbative calculation becomes too small[2] and a new mechanism has to be invoked to describe the process. As z becomes close to 1, the proton is disturbed less and less by the gluon emission, and the interaction between the upper quarks of figure 2a and the proton becomes softer and softer. This is the regime where our model should be valid. In fact, for inclusive distributions, it has been shown that, at small x, the gluon distribution is well reproduced by the emission of gluons with a modified propagator[6]. So at high z, we can replace the gluon structure function of figure 2a by the emission of a modified gluon. For exclusive distributions, one now needs to decide how to deal with the final state gluons. As the vector meson is assumed to be made of valence quarks only, one has to branch them back into the proton, thus obtaining figure 2b (diagrams for which the gluons couple to different quarks in the proton are suppressed in this model, see ref. 1). Our calculation is thus equivalent to a perturbative QCD model with a definite prescription for the absorption of final state gluons by the proton: the emission and the absorption are treated on an equal footing. This reabsorption mechanism is not included in the usual perturbative QCD analysis, so that the latter is too small at high z.

From the $\nu \rightarrow \infty$ limit of the diagrams of fig. 2b, one can see that t-channel analyticity implies that the amplitude is pure imaginary. It can thus be evaluated by cutting the first two diagrams of fig. 2b. All quark lines are then on shell, except those designated by a dot in the upper bubble. Both are far off-shell, by amounts z_1 and z_2 of the order of Q^2. We assume that they couple to the gluon via a perturbative coupling, taken at a scale $\Sigma^2=Q^2$ or $\frac{1}{2}(z_1+z_2)$. In the limit $\nu \rightarrow \infty$, the amplitude is then:

$$A = i\frac{8\sqrt{2}}{3\pi} m_V \sqrt{\frac{\alpha_s(\Sigma^2)}{\alpha_n}}\, \wp \int_{-\infty}^{0} dl^2 \frac{-4l^2 + t}{(m_V^2 + Q^2 - t)(-4l^2 + Q^2 + m_V^2)} [4\pi\alpha_n D(l^2 + \tfrac{t}{4})]^2 \qquad (5)$$

$\wp$ is a term depending on the polarizations ε and e of the photon and of the vector meson respectively, and is given by $\wp=(q^\alpha \varepsilon\cdot e - \varepsilon^\alpha e\cdot q - e^\alpha \varepsilon\cdot V) P_\alpha$. In the large ν limit, this model conserves helicity so that transverse photons produce transverse vector mesons, and the same for longitudinal ones. One can derive for large ν that $\wp_T = \frac{w^2}{2}$ and $\wp_L = \frac{w^2}{2}\left(\frac{t + m_V^2 + Q^2}{2m_V\sqrt{Q^2}}\right)$.

One more ingredient needs to be added in the case of elastic production. One still needs to exclude the possibility for the scattered quarks to fragment into p + kπ, n*+kπ... instead of one single proton. One uses here the fact that the exchange of two modified gluons effectively behaves like photon exchange[1]. This means that in this case, as for the photon, the amplitude corresponding to the probability that the proton interacts elastically is given by the measured proton elastic form factor:

$$F_1(t) = \frac{4m_p^2 - 2.8t}{(4m_p^2 - t)(1 - \frac{t}{0.7})^2} \tag{6}$$

$3F_1$ can be thought of as the overlap between the wave functions of the incident and of the scattered protons, and needs to multiply the amplitude (5).

Finally, higher-order corrections can be approximately included by making use of the analogy with pomeron exchange: whereas two-gluon exchange predicts a pomeron trajectory 1+0 t, the real one is 1+0.08+$\alpha' t$, with α'=(2 GeV)$^{-2}$. Expecting the same effect here that in the case of the hadronic cross section, one can the multiply the amplitude (5) by:

$$Z = \left(\frac{w^2}{w_0^2}\right)^{0.08+\alpha' t} \tag{7}$$

with $w_0^2 \approx 1/\alpha'$.

Summing it all up, the formula for the differential cross section becomes:

$$\frac{d\sigma}{dt} = \left[\frac{\alpha_{elm}}{4w^4}|A|^2\Phi^2\right] Z^2 [3F_1(t)]^2 \tag{8}$$

with α_{elm} the electromagnetic coupling constant. This formula can be approximately integrated if one fixes the l^2 term in the denominator of (5). This integral then gives:

$$\int dl^2 \approx \frac{\beta_0^2(\mu_0^2 + t/2)}{(m_v^2 + Q^2 - 4l^2)(m_v^2 + Q^2 - t)} \tag{9}$$

This provides the connection with the model based on pomeron exchange by Donnachie and Landshoff[3]. The expression (9) is essentially identical to the corresponding one in ref. 3, except for the $t/2$ term in the numerator. This means that (8) has a bigger t slope than in the pomeron case and that the integrated cross section will be smaller. We can also see from (8) and (9) that the exact form of the propagator is not too important, and that the result will essentially depend on (1) and on $\int_{-\infty}^{0} dz\, z\, D^2(z)$. Previous study[4] has shown that this second integral is very well constrained by (2). Equation (9) also shows that the leading ν approximation breaks down for $t=2\mu_0$.

Before turning to a detailed comparison with the data, figure 3 gives the prediction of the model for various μ_0^2 at ε=0.85 and w^2=150 GeV^2. The uncertainty due to the choice of scale in α_S is shown in the middle curve. Using α_n as in figure 1 reduces the uncertainty from Λ_{QCD} to a few percent. The model reproduces the Q^2 dependence of the cross section remarkably well, and from these data, one can determine μ_0^2= 1.2±0.5 GeV^2. This agrees very well with the previous estimate (2) based on condensates, which we shall use in the following. The error on μ_0^2 amounts to an overall normalization uncertainty of a factor 2 either up or down. One can also see that the cross section is not well reproduced at low Q^2. This is due to two separate effects: i) the approximate form of the ρ^0 vertex (4) breaks down at very low Q^2, typically of the order of the transverse momentum of the quarks bound in a ρ; ii) as the scale is decreased, the quark propagator of the off-shell quarks of fig. 2b should be modified in a way similar to the gluon propagator. The lowest Q^2 scale at which the agreement is still reasonable is 0.5 GeV^2, and corresponds to a quark off-shellness $Q_q^2 \approx$ 0.21 GeV^2. This seems to confirm[6] that for light quarks the scale at which the quark propagator should be modified is indeed much lower than the scale controlling the gluon propagator.

2. Comparison with data and inelastic background

We now turn to an explicit comparison with the EMC hydrogen data[7,9]. One needs to write the muon cross section in terms of the virtual photon cross section (8). This is a standard technique in deep-inelastic scattering[10]. Let us simply remind the reader of the main formulae:

$$\frac{d\sigma}{dQ^2 d\nu} = \Gamma[\sigma(\varepsilon_T, e_T) + \varepsilon\sigma(\varepsilon_L, e_L)]$$

$$\text{with} \quad \Gamma = \frac{\alpha_{elm}(\nu - \frac{Q^2}{2m_p})}{2\pi Q^2 E^2 (1-\varepsilon)} \tag{10}$$

$$\text{and} \quad \varepsilon = \left\{1 + \frac{2(Q^2 + \nu^2)}{4EE' - Q^2}\right\}^{-1}$$

with E and E' the energies of the incident and of the scattered muons. To remain as close as possible to the experimental procedure, as outlined in ref.11, a simple Monte Carlo simulation based on (10) has been written. It generates $\frac{d\sigma}{dQ^2 d\nu}$ in 6 Q^2 bins (3-7, 7-10, 10-13, 13-16, 16-19, 19-25) GeV^2 and 6 ν bins (0-50, 50-65, 65-90, 90-130, 130-150, 150-240) GeV. The EMC cuts at E=280 GeV[7] are

implemented, i.e. 36 GeV^2<w^2<360 GeV^2, θ>8 mrad, E'>40 GeV. One then calculates a correcting factor for each bin, by running the program with and without cuts. After correcting for these, one can extract the photon cross section as a function of Q^2,ν using (10). We perform a background analysis following exactly the same method for the extraction of the photon cross section and performing the same corrections for cuts.

The main signature for elastic events is the observation of two and only two hadrons in the ρ^0 mass region with momentum bigger than 3 GeV. The cut which removes most of the inelastic background is on the inelasticity $I=\frac{[q+p-V]^2-p^2}{w^2}$, which is constrained to lie in [-0.1,0.08] (I=0 for elastic events before experimental smearing). The proton is not directly observed, so that p+nπ states are not a priori ruled out. In the NA9 phase of the experiment, EMC have lowered the minimum hadron energy to 200 MeV and observed 4 events out of 28 with pion contamination, i.e. the inelastic background made of hadrons between 0.2 and 3 GeV is at least (14 ± 6)%.

The inelastic background, so constituted of events with only two hadrons going through the cuts, needs to be evaluated via a Monte Carlo which will produce reasonable multiplicity distributions in deep-inelastic scattering. EMC used the string-based Lund Monte Carlo[12] for the evaluation of their background, so that, to have an idea of the uncertainties involved, we have chosen to use the Marchesini-Webber HERWIG Monte Carlo[13]. In its latest version, it includes deep-inelastic photon scattering and is well suited for our purpose. The fragmentation proceeds via a cluster model: the final-state partons are grouped into colour singlet clusters which are decayed according to their mass: high mass ones go into two collinear smaller mass clusters, while low-mass ones are left to decay isotropically into two hadrons. Very-low mass clusters are allowed to turn into a single hadron, and the remaining energy is transferred to a neighbouring cluster. This enables HERWIG to reproduce adequately the high-z events in e^+e^-.

We want to stress here that the results produced by such programs based on the QCD improved parton model are only qualitative. The semi-exclusive character of the distributions, and their low Q^2, reduce gluon radiation to a minimum, so that all the knowledge that has been accumulated about this in the last years[14] is of little use here: the distributions must be highly dependent on the fragmentation algorithm used. Moreover, the high-z region is artificially reproduced in current fragmentation models, and the answer should only be considered as an ansatz working in electron-positron collisions. Finally, the events are at low x, where the input distribution functions are not very well known.

As a first test of this background evaluation figure 4 shows the inelasticity distribution generated by HERWIG and compares it with the LUND prediction as calculated by EMC[7, 9]. The uncertainties come from varying the cluster mass cutoff from 1 to 4 GeV and from varying the input structure functions. We have not included experimental smearing, so that the HERWIG curves are not depleted near I=0, as the LUND curve, which has been folded with the experimental resolution. We insist that a Monte Carlo simulation cannot produce a single curve, especially in this very poorly known region of phase space.

To illustrate the uncertainties attached to the Monte Carlo evaluation of the inelasticity distribution, let us mention that another Monte Carlo, SHERIE[15], which uses essentially the same physics as HERWIG, fails to reproduce the inelasticity distribution observed by EMC. The prediction is that a flat distribution is generated, from I=0 to 0.2, giving an enormous background to exclusive events. This Monte Carlo is, however, very successful in its prediction of other distributions and has been tuned to reproduce most of the EMC data[16].

Furthermore, accumulating enough statistics via a generic Monte Carlo simulation is not a trivial task: of the order of 1 event out of 1000 contributes to the elastic distributions after cuts. For the evaluation of the Q^2 dependence of the background, one needs to split the integral in several Q^2 regions, as the distribution is very peaked. This is unfortunately not possible to do in the case of the t distribution. We shall come back to that point later.

3. Results

Table 1 shows the averages and cross sections both for the background and the signal. One has to be careful in interpreting the theoretical error bars. They only show a range of possibilities and their central value is not preferred in any sense. The uncertainty in the model predictions come from varying Λ_{QCD} between 0.1 and 0.35 GeV and from the choice of scale in α_S. The photon cross section corresponds to our first Q^2 bin, extrapolated from $\langle Q^2\rangle$≈4.5 GeV^2 to 2 GeV^2, assuming the $(1+\frac{Q^2}{m_V^2})^2$ dependence used for the data. One sees that there is general good agreement, and that the background is calculated to be (20 ± 6) %. HERWIG predicts that 1/8 of the events will have both hadrons with energy smaller than 0.2 GeV, so that (17±5) % of the data is inclusive, for hadrons detected between 0.2 and 3 GeV. This is to be compared with the minimum (14±6)% derived above from the EMC checks. The experimental averages are not corrected for acceptance, but the comparison is meaningful

in the ν and ε case as the acceptance is almost flat for these two variables. This is not the case for Q^2, so that we do not show the raw experimental number.

Figure 5 shows the Q^2 dependence of the photon cross section. The agreement with data is very good, and one sees that the inclusion of the background improves the agreement at high Q^2: the inclusive background falls slower than the signal. Notice that the cross section falls faster than $(1+\frac{Q^2}{m_V})^2$ which is the form used by EMC in their extrapolations. We also want to point out that the experimental errors in this figure and the following ones are only statistical, and do not include an additional 25% systematic error on the absolute normalization, and a 15% possible mismatch between data sets at different energies.

Figure 6a shows the photon cross section as a function of ν. This quantity is extracted for each bin in (Q^2,ν), and for each ν the various Q^2 bins are extrapolated to Q^2=5 GeV^2, and then averaged. We use the same ρ-propagator extrapolation as was used for the data. This means that the high Q^2 bins will contribute too little to the average, which in turn will be smaller than the true model prediction. In our case, this leads to a mismatch between the real and the extrapolated values of a factor 2. Moreover, we want to point out that $1/(1-\varepsilon)$, which comes as a factor in the extraction of the photon cross section from the muon one, see (10), depends highly on ν:

for $\nu \to \infty$

$$\frac{1}{1-\varepsilon} \approx 1 + \frac{2\left(1-\frac{\nu}{E}\right)}{\left(\frac{\nu}{E}\right)^2} \qquad (11)$$

This goes from 1 to 130 as ν goes from 40 to 280 GeV. This means that an uncertainty in the value of ν used in each ν bin might lead to a big error in the photon cross section.

At fixed energy, for each ν bin, $\langle\varepsilon\rangle$ is essentially constant, see (11). Figure 6a can thus be translated into figure 6b. (The experimental points have been corrected for the change in energy between them). Again, the Q^2 extrapolation leads to a result which is too small and binning dependent. We give for reference the real model prediction at Q^2=5 GeV^2 for Λ_{QCD}=0.1 GeV and $\Sigma^2=Q^2$. Our model leads to essentially a straight line $\sigma(\varepsilon)=\sigma_T+\varepsilon\,\sigma_L$, with a positive slope. The EMC data are marginally consistent with the real model prediction.

However, from these and low Q^2 data previously obtained by the CHIO collaboration[17], EMC conclude that the longitudinal cross-section is consistent with zero. The argument is as follows: the

CHIO data are at $\langle\varepsilon\rangle\approx$0.39, and after correcting for their different $\langle\nu\rangle$, they are extrapolated from $Q^2\approx$0.66 GeV^2 to 2 GeV^2, using a ρ propagator dependence. This leads to σ_γ^{CHIO}(2 GeV^2) = (468±48) nb (the statistical and the systematic errors have been added in quadrature). As this is higher than the value measured by EMC at $\langle\varepsilon\rangle\approx$0.85, the conclusion is that σ_L is consistent with zero.

Here the extrapolation plays a crucial role. If it is assumed that the very low Q^2 data are well fitted by the ρ propagator, but that above 1 GeV^2 the functional form changes to the square of (9) (with t=0 and $l^2\approx\mu_0^2/2$), σ_γ^{CHIO} becomes (25.1±2.57) nb at Q^2=5 GeV^2. The EMC measurement at 280 GeV then becomes (70.5±9.1) nb when extrapolated to the same Q^2. This is in perfect agreement with Figure 6b. Unfortunately this exercise cannot be totally satisfactory, as the above-mentioned binning effects cannot be taken into account and must be important when dealing with the data as a whole. Also, the number for the extrapolated CHIO cross-section is very sensitive to the scale Q^2 at which (9) becomes valid. But one can see that the measurement of a negligible σ_L, and the subsequent claim of non conservation of helicity can be related to the form used in the Q^2 extrapolation of low-energy data.

From the measurement of the decay distribution of ρ mesons, one can extract their polarization. One can then obtain the ratio $R=\sigma_L/\sigma_T$ assuming s-channel helicity conservation. Figure 7a shows the data together with the prediction of our model for the same parameter choices as in figure 6b. There is reasonable agreement, except at high Q^2, where we have not included the background contribution. This background is concentrated at high ε, thus increasing R. Figure 7b shows r_{00}^{04}, the probability to produce longitudinal ρ mesons averaged over the photon polarization, which we compare with $\frac{\varepsilon\,\sigma_L}{\sigma_T+\varepsilon\,\sigma_L}$. Again, one sees that reasonable agreement is reached.

We now turn to the most puzzling feature of the data: the differential distribution $\frac{d\sigma}{dt'}$, with t' the difference between t and its kinematic minimum. This has been fitted by EMC to a form $e^{-bt'}$. Assuming such a dependence, one gets $\langle t'\rangle$=1/b. Figure 8a shows the prediction of the model, the background and the data. The background estimate is corrected to take into account the difficulty of extracting a peaked distribution via a Monte Carlo study. The error bars include our estimate of the systematic error resulting from this. Nevertheless, the disagreement is striking.

One can first consider the possibility that the background is underestimated at high Q^2. As the EMC checks are for total event rates, and as the distribution is highly peaked with Q^2, one could consider a background much bigger than that predicted by HERWIG at high Q^2. This would produce a

t' distribution made of a peak followed by a flat part, which does not seem to be the observed shape. Moreover, as the disagreement is for all Q^2, this rather desperate method would not help very much. One must rather look for an overall explanation, valid for all Q^2.

The source of the disagreement in this model is clear, however, and has already been pointed out by EMC themselves. In references 7 and 9, it is asserted that the data are well fitted by a photon-gluon fusion model. But such a model does not include any factor such as $F_1(t)$. No matter what the model is, one cannot assume that a proton submitted to a momentum transfer t always remains a single proton. As t increases, it is clear that this possibility is more and more unlikely. Thus the only alternative is that the data are well fitted because they are inclusive.

This "semi-exclusive" character of the data, already considered in ref. 9, is confirmed by i) the background slopes, which are consistent with the data; ii) figure 8b which shows the slopes that would result from our model summed with the background in two cases: when the elastic form factor of the proton is set to 1, and when both this factor and the factor Z of (5) from higher orders are set to 1. This clearly illustrates that the slopes are not linked to a particular model, but rather to inclusive distributions: the disagreement arises, not from our model, but rather from the inclusion of the proton wave-function overlap. In the inclusive version of our model, all the other results would still hold, except that the central value of μ_0 would need to be reduced. For such an explanation to be valid, one would need to make most of the events inclusive, i.e. the proton fragmentation should be such that almost all events make it through the cuts, i.e. are composed of extremely soft mesons, or photons.

Another possibility would be to assume that the process does not factorize, i.e. that the ρ is not produced at small distances, but this would essentially prohibit any interpretation based on photon-gluon fusion, and would make the other successes of the model an even greater puzzle.

4. Conclusion

Taken at face value, the data seem to point out to an inclusive process that violates helicity and that can hide its inclusive character within the EMC cuts. We have argued that the violation of helicity could probably be ascribed to experimental uncertainties. The inclusive character of the t slopes seems on the other hand much harder to dispose of and it seems that the EMC data show that in diffractive processes protons emit extremely low momentum particles, more then half of them below 200 MeV. It would be very interesting to see whether these features can be reproduced at higher energies: measuring

$\langle t \rangle$ as a function of Q^2 at NMC might turn out to be essential in our understanding of soft physics, and such a measurement at HERA would provide further information on the x_B dependence of the phenomenon.

On the theoretical side, the idea that the gluon propagator needs to be modified at small momentum transfer seems to be fruitful, and enables one to extend perturbative QCD to small momentum transfers. The ensuing model provides reasonable agreement with the data both for the ratio σ_L/σ_T and for the Q^2 dependence of the cross section. We want finally to conclude that the constraints put on this model in an earlier paper [6] seem to be confirmed. We also got some information on the light quark propagator, which seems to change at much smaller scales than the gluon.

Acknowledgements

I am indebted to P.V. Landshoff for his help and suggestions and to K. Hamacher for correcting several of my misinterpretations of the data, for his patient explanations and fruitful suggestions. I also want to acknowledge discussions with T. Sloan, B.R. Webber, A. Donnachie and H.R. Wilson. I thank the High Energy Physics group at the Cavendish Laboratory for letting me use their facilities.

References

1. P.V. Landshoff and O. Nachtmann, Z. Phys. **C35** (1987) 405.

2. R. Baier and R. Rückl, Nucl. Phys. **B201** (1982) 1.

3. A. Donnachie and P.V. Landshoff, Phys. Lett. **185B** (1987) 403.

4. A. Donnachie and P.V. Landshoff, Nucl. Phys. **B311** (1989) 509.

5. D. Ross, Southampton preprint SHEP 88/89-9 (1988).

6. J.R. Cudell, A. Donnachie and P.V. Landshoff, Nucl. Phys. **B322** (1989) 55.

7. EMC Collaboration, J.J. Aubert et al., Phys. Lett. **161B** (1985) 203; J. Ashman et al., Z. Phys. **C39** (1988) 169.

8. R.R. Horgan, P.V. Landshoff and D.M. Scott, Phys. Lett. **110B** (1982) 493.

9. K. Hamacher, Ph. D. Thesis, Wuppertal preprint WU B-DI 84-2 (1984).

10. F. Halzen and A.D. Martin, Quarks and Leptons (John Wiley & sons, New York: 1984), p. 186.

11. EMC, J.J. Aubert et al., Nucl. Phys. **B213** (1983) 1.

12. G. Ingelman et al., Nucl. Phys. **B206** (1982) 239.

13. G. Marchesini and B.R. Webber, Cavendish preprint HEP-87/9 (1987).

14. G. Marchesini and B.R. Webber, Nucl. Phys. **B310** (1988) 461.

15. H.R. Wilson, Cavendish preprint HEP-88/8 (1988); Nucl. Phys. **B310** (1988) 589.

16. H. Wilson, Ph. D. Thesis (1988), p. 47.

17. CHIO Collaboration, W.D. Shambroom et al., Phys. Rev. **D26** (1982) 1.

Table 1: averages and cross sections

The muon cross section is integrated for Q^2=3 to 25 GeV^2 and the photon cross section is extrapolated at Q^2=2 GeV^2 (see text). All quantities are for E=280 GeV.

Quantity	$\langle Q^2 \rangle$ (GeV^2)	$\langle \nu \rangle$ (GeV)	$\langle \varepsilon \rangle$	σ_γ (nb)	σ_μ (pb)	statistics
Model	5.59 ± 0.06	91.3 ± 0.5	0.895±0.001	395±30	200 ± 15	200000
Background	4.9 ± 0.5	45.8 ± 0.2	0.970±0.002	51 ± 8	49 ± 10	172 / 124
Total	5.45 ± 0.12	82 ± 0.5	0.910±0.001	446 ± 38	249 ± 23	–
EMC data	--	97	0.85	396±51	--	170

Figure Captions:

Figure 1: The scale (a) and coupling constant (b) at which the non perturbative gluon propagator crosses the perturbative one. The three curves are for three different values of μ_0^2 indicated (in GeV^2) next to the curve.

Figure 2: (a) Photon-gluon fusion diagram contributing to the inclusive cross-section.
(b) The three diagrams leading to equation (5). The quark that remains off-shell in (5) is indicated by a dot.

Figure 3: The photon exclusive cross-section as a function of Q^2. The three curves correspond to various values of μ_0^2 indicated (in GeV^2) next to the curve. The two curves for μ_0^2=1.2 GeV^2 show the uncertainty attached to the choice of scale in α_S. The data is from EMC and other groups, see ref. 7.

Figure 4: The inelasticity distribution for events containing two detected hadrons. The raw prediction of HERWIG is compared with that of LUND (smeared with the experimental resolution) and with the EMC data.

Figure 5: The photon cross-section as a function of Q^2, including our background estimate, is compared with the EMC data of ref. 7.

Figure 6: The photon cross-section, extrapolated at Q^2=5 GeV^2 and averaged (see text), is compared with data from ref. 9, and plotted as a function of $\langle \nu \rangle$ (a) and of $\langle \varepsilon \rangle$ (b). (b) also shows the cross section predicted by our model at 5 GeV^2 without extrapolation and without including the background. The key to this graph is the same as that of figure 5.

Figure 7: The ratio $R = \frac{\sigma_L}{\sigma_T}$ (a) and the probability r_{00}^{04} to produce a longitudinal ρ^0 (b) are compared with the prediction of our model.

Figure 8: (a) The slopes of the t' distribution, from ref. 7 are compared with the prediction of our model, including the background estimate. The error on the background allows for systematics (see text). The key to this graph is the same as that of figure 5.
(b) The same data are compared with the prediction of our model for inclusive distributions, including the Monte Carlo background as in (a).

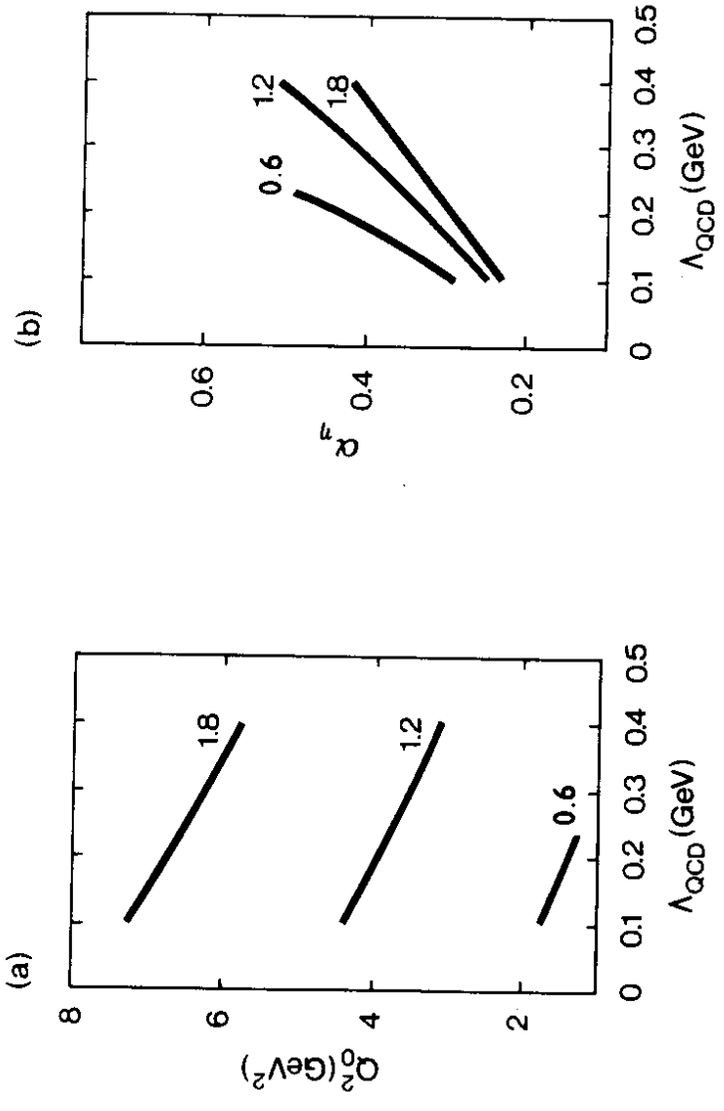

Figure 1

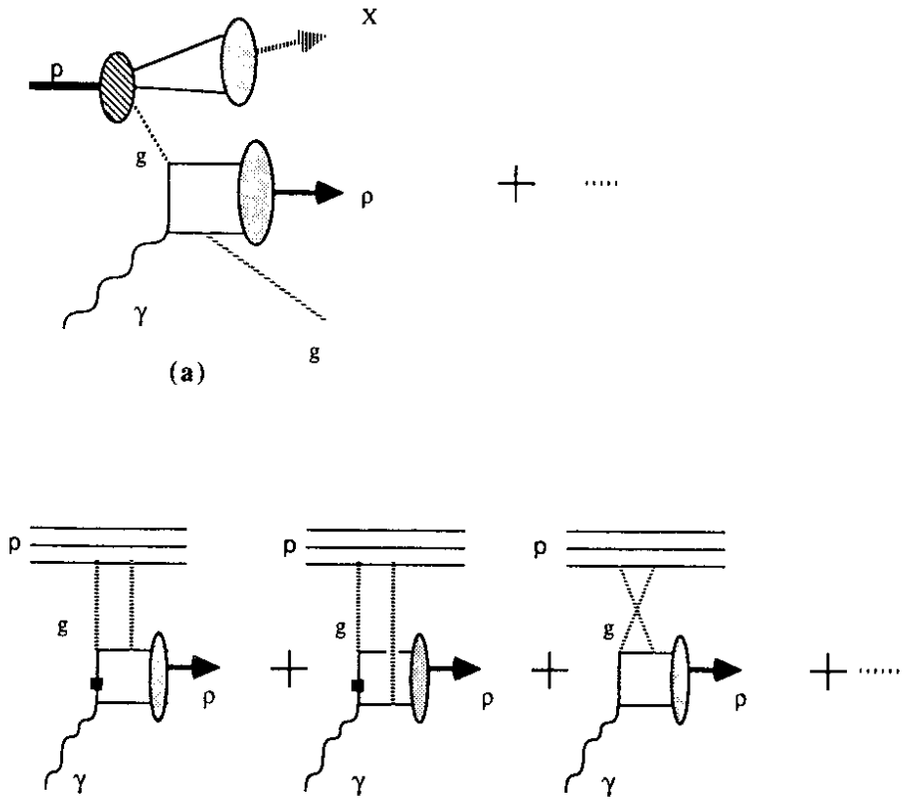

Figure 2

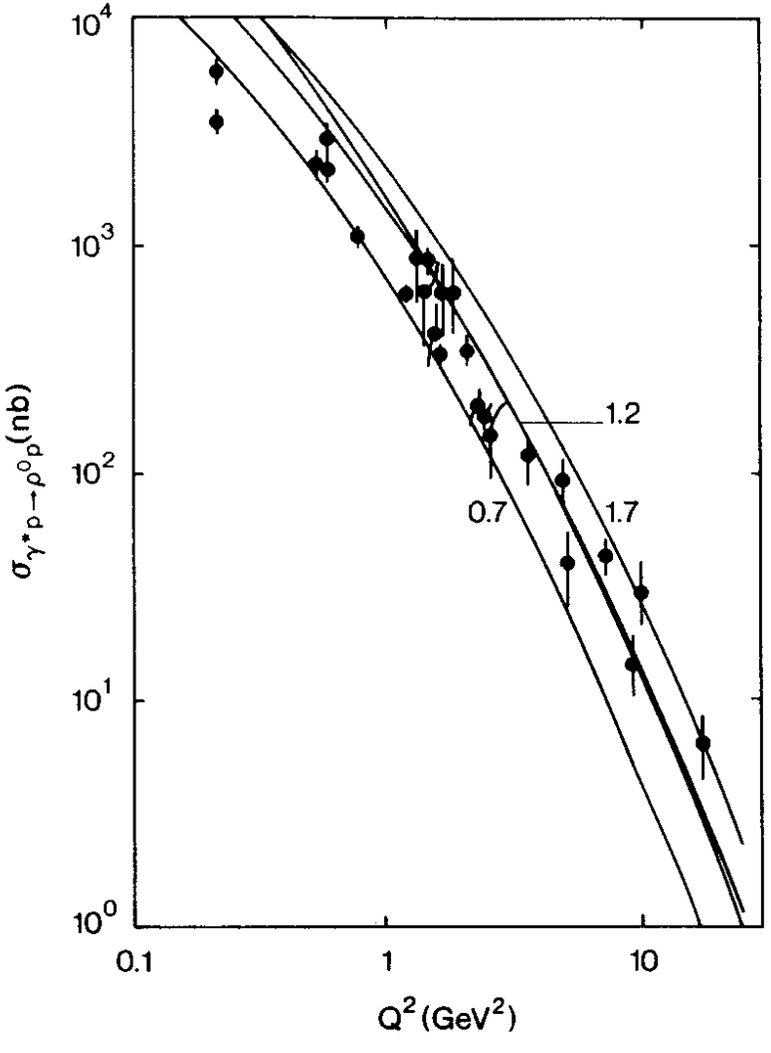

Figure 3

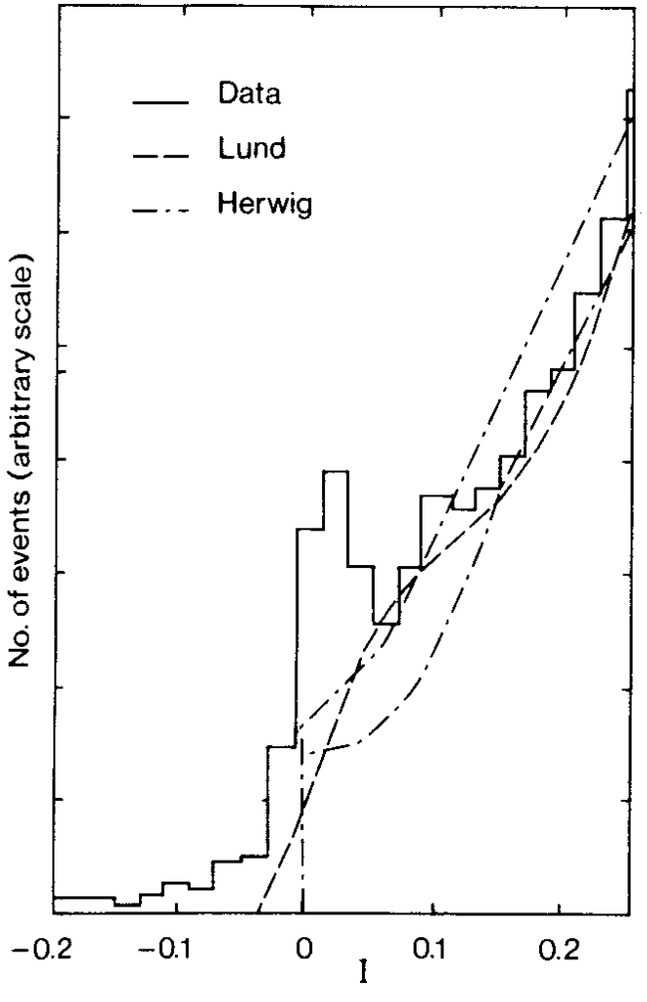

Figure 4

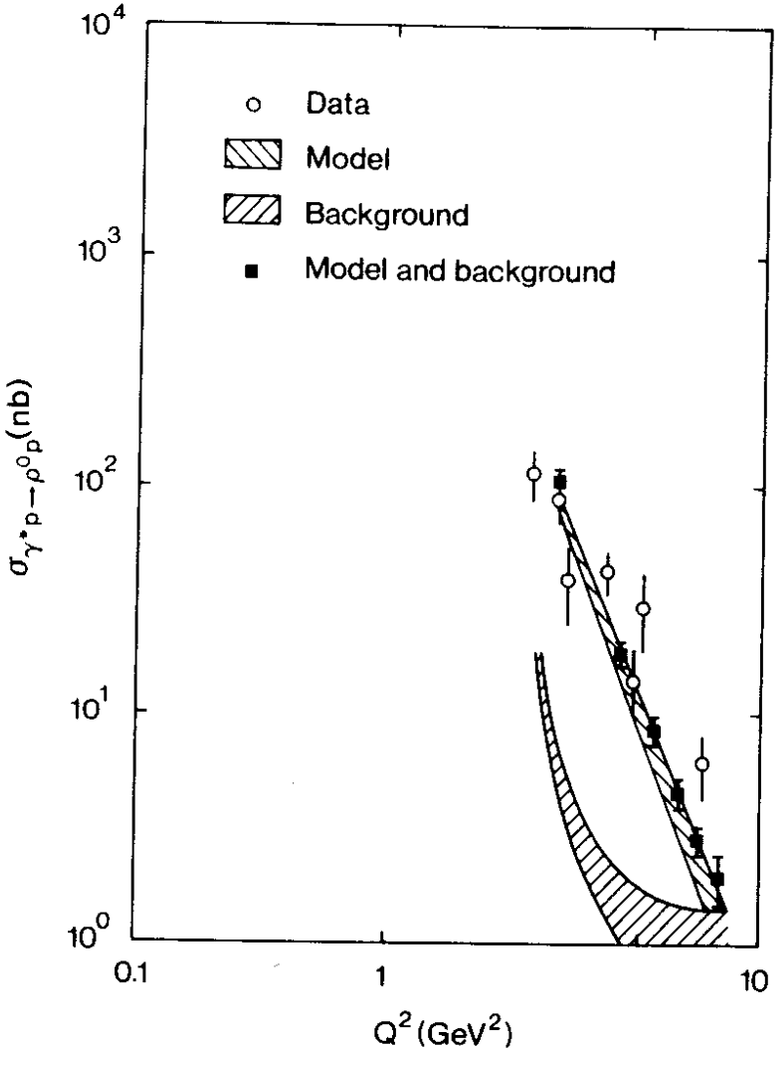

Figure 5

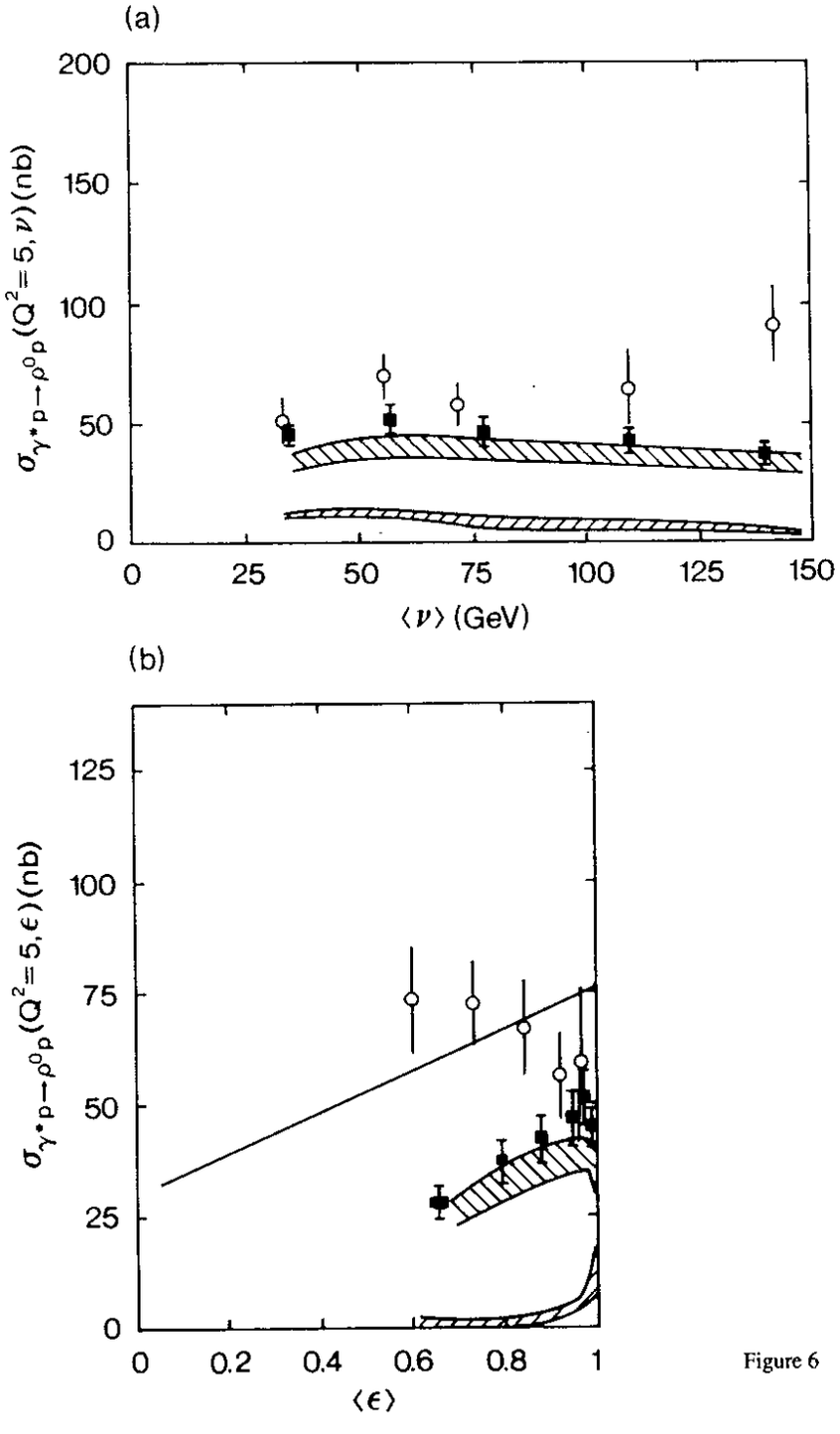

Figure 6

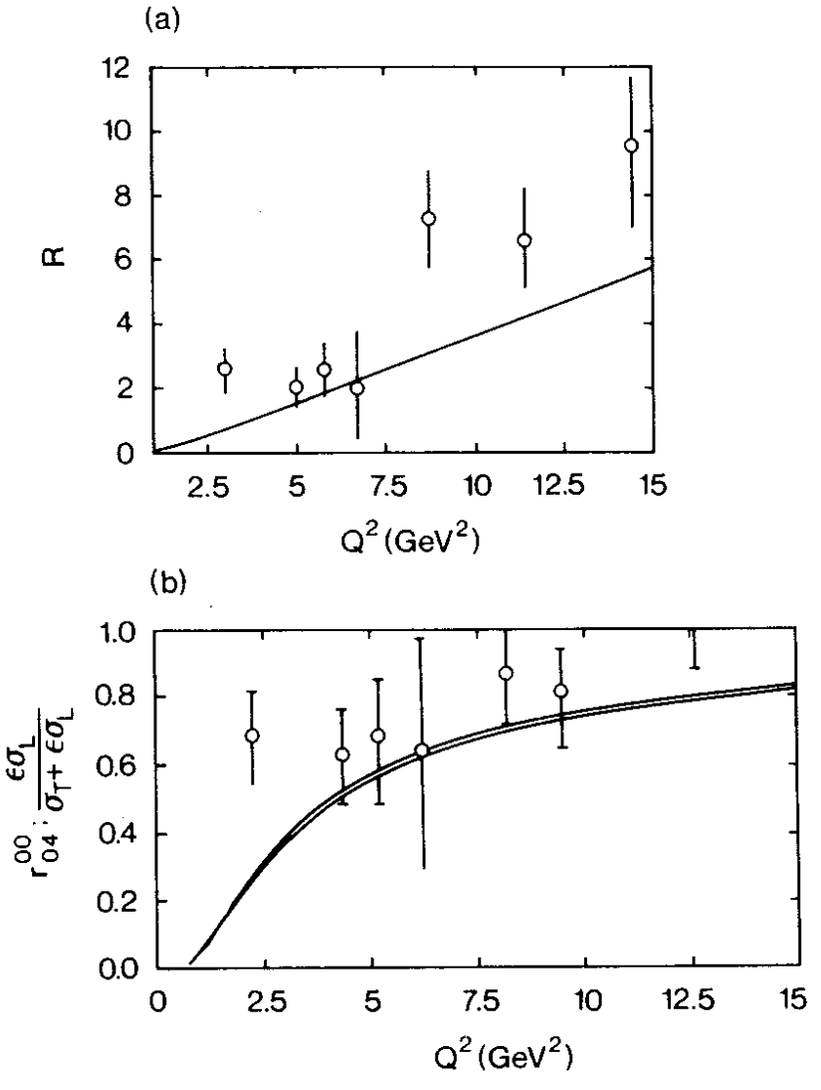

Figure 7

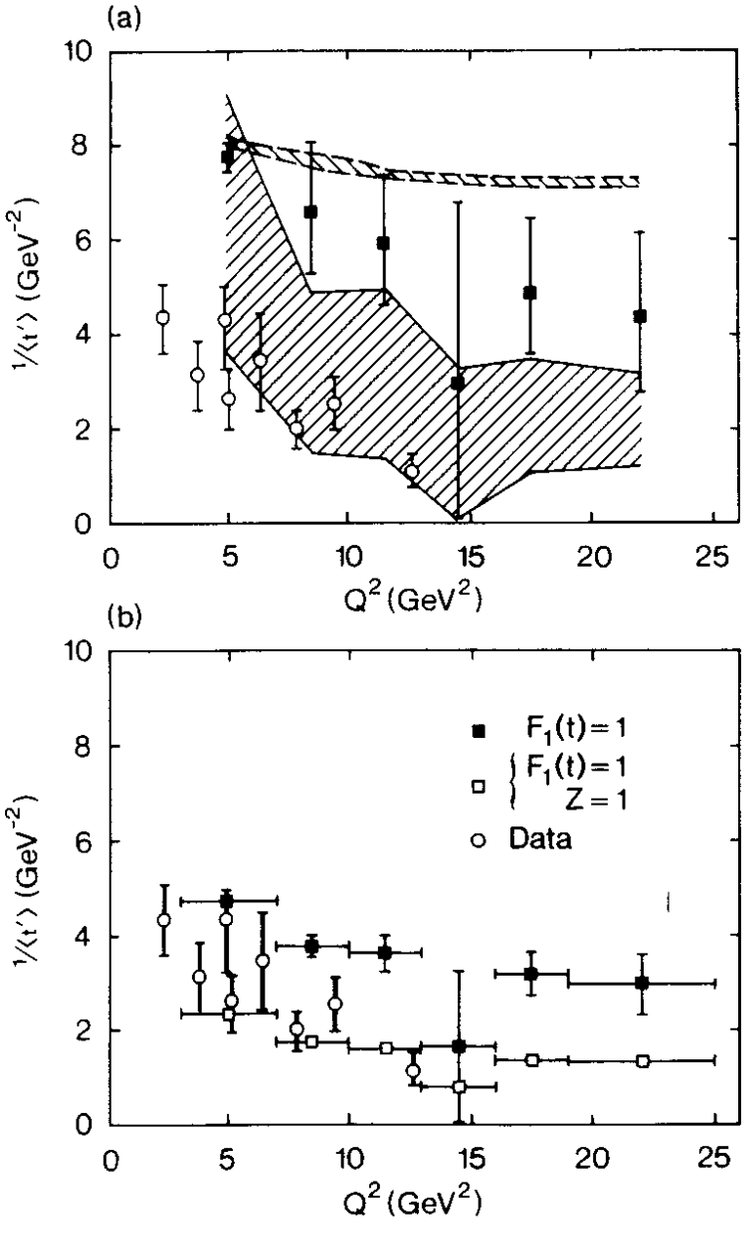
(a)
10
8
6
4
2
0
0
5
10
15
20
25
$1/\langle t' \rangle$ (GeV^{-2})
Q^2 (GeV^2)
(b)
$F_1(t)=1$
$F_1(t)=1$
$Z=1$
Data
$1/\langle t' \rangle$ (GeV^{-2})
Q^2 (GeV^2)

Figure 8